research. Acknowledgment is also made to the donors of the Petroleum Research Fund, administered by the American Chemical Society, for partial support of this research. We also thank the University of Tennessee Computer Center for their continuing support and patience.

References and Notes

(1) Gurler, M. T., Crabb, C. C.; Dahlin, D. M.; Kovac, J. *Macromolecules* **1983**, *16*, 398.
(2) Kranbuehl, D. E.; Verdier, P. H. *J. Chem. Phys.* **1979**, *71*, 2662 and references therein.
(3) Rouse, P. E. *J. Chem. Phys.* **1953**, *21*, 1273.
(4) de Gennes, P. G. "Scaling Concepts in Polymer Physics"; Cornell University Press: Ithaca, NY, 1979.
(5) Crabb, C. C.; Kovac, J. *Macromolecules* **1985**, *18*, 1430.
(6) Verdier, P. H. *J. Chem. Phys.* **1966**, *45*, 2118.
(7) Verdier, P. H. *J. Chem. Phys.* **1973**, *59*, 6119.
(8) Hilhorst, H. J.; Deutch, J. M. *J. Chem. Phys.* **1975**, *63*, 5153.

Steady-State Compliance of Linear Polymer Solutions over a Wide Range of Concentration

Yoshiaki Takahashi,* Ichiro Noda, and Mitsuru Nagasawa

Department of Synthetic Chemistry, Nagoya University, Furo-cho, Chikusa-ku, Nagoya 464, Japan. *Received February 13, 1985*

ABSTRACT: Measurements of zero-shear viscosity $\eta°$ and steady-state compliance J_e of linear polystyrenes with high molecular weights were carried out in good and poor solvents with a Weissenberg rheogoniometer to examine the applicability of the scaling theory of de Gennes to J_e. It was confirmed, in agreement with a previous work, that the experimental data of $\eta°$ in semidilute solutions agree with predictions of the scaling theory. However, the scaling theory did not agree with the experimental data of J_e. It was concluded that the idea of a semidilute region need not be brought in to understand J_e of linear polymer solutions.

Introduction

Theories of the molecular weight (M) and polymer concentration (C) dependences of the zero-shear viscosity $\eta°$ of linear polymers[2,3] as well as of their osmotic pressure Π[4] are based on quite different models in dilute and concentrated solutions. It was reported[1,5-7] that the gap between the theories for dilute and concentrated solutions can be filled if we recognize the existence of so-called semidilute solutions as proposed by de Gennes.[8] In the semidilute region it is assumed that the polymer coils overlap each other but the segment density is still so low that the excluded volume effect works between segments. Also, the polymer concentration dependence of a property in semidilute solution can be predicted by the scaling method of de Gennes.[8]

That is, if we define a viscosity parameter $\eta_R°$ by

$$\eta_R° \equiv \eta_{sp}°/C[\eta]$$

where $\eta_{sp}° = (\eta° - \eta_s)$, η_s is the solvent viscosity, and $[\eta]$ is the intrinsic viscosity, $\eta_R°$ of semidilute solutions is given by[1]

$$\eta_R° \propto (C/C^*)^{(4.4-3\nu)/(3\nu-1)} \quad (1)$$

or

$$\eta_{sp}° \propto M^{3.4}C^{3.4/(3\nu-1)} \quad (2)$$

where $C^* = 3M/(4\pi\langle S^2\rangle^{3/2}N_A$ is the critical concentration at which polymer coils begin to overlap each other and ν is an excluded volume exponent defined as $\langle S^2\rangle \propto M^{2\nu}$. $\langle S^2\rangle$ is the mean square radius of gyration and N_A is Avogadro's number. In dilute solutions, $\eta_R°$ is given by

$$\eta_R° = 1 + k(C/C^*) + \ldots \quad (3)$$

where $k = 3km\Phi/4\pi N_A$ and k' and Φ are the Huggins constant and the Flory coefficient, respectively. It was reported in a previous paper[1] that the predictions of eq 1–3 are in agreement with the experimental data of poly(α-methylstyrenes) (PαMS) in good solvents as well as in Θ solvents if the molecular weights of the polymers are sufficiently high.

The viscoelastic properties of polymer solutions of melts, however, can be described by two parameters expressing the energy dissipation and storage mechanisms, such as zero-shear viscosity $\eta°$ and steady-state compliance J_e. The purpose of this work is to examine whether or not the concept of the semidilute region is useful for understanding not only $\eta°$ but also J_e over the entire range of polymer concentrations. The molecular weight and polymer concentration dependences of the steady-state compliance J_e of linear polymers are also different in different regions.[2,3] If the polymer concentration is below a certain value, J_e becomes proportional to M/C, in agreement with the modified Rouse theory for the viscoelastic properties of unentangled polymers. We call this region the Rouse region in this paper, though the original Rouse theory should be applied to infinitely dilute solution. If we define J_{eR} by

$$J_{eR} \equiv [J_eCRT/M][\eta°^2/(\eta° - \eta_s)^2]$$

J_{eR} is a constant independent of molecular weight and polymer concentration in the Rouse region. The constant is ~0.4 in good solvents and higher in poor solvents. In concentrated solutions or in melts, on the other hand, the polymer molecules are extensively entangled with each other so that all entanglement points are distributed uniformly in the solution. Then the entanglement density is proportional to C^2, and J_e should be proportional to C^{-2} independent of M and the solvent if the conformation of the polymer chain between two adjacent entanglement points is Gaussian. That is

$$J_e \propto C^{-2} \quad (4)$$

or

$$J_{eR} \propto (CM)^{-1} \quad (5)$$

The region is often called the network region. These speculations were found to agree with experimental data

0024-9297/85/2218-2220$01.50/0

Table I
Molecular Characteristics

sample code	$M_w \times 10^{-6}$ [a]	M_w/M_n [a]	$C^* \times 10^3$, g/mL good [b]	$C^* \times 10^3$, g/mL θ [c]	$[\eta]$ good [d]	$[\eta]$ θ [e]
F-2000	20.6		0.45_0	0.37_2	23.0_7	3.6_8
F-850	8.42	1.17	0.89_6	0.58_4	12.0_1	2.3_5
F-450	4.48	1.14	1.5_4	0.80_2	7.5_7	1.7_1
F-128	1.26	1.05	3.9_7		2.9_6	
F-80	0.775	1.01	5.8_0		2.0_7	

[a] Reported values from manufacturer. [b] In good solvents[7] $\langle S^2 \rangle = 1.38 \times 10^{-18} M^{1.19}$. [c] In θ solvents[29] $\langle S^2 \rangle = 8.18 \times 10^{-18} M$. [d] In good solvents[7] $[\eta] = 9.06 \times 10^{-5} M^{0.74}$. [e] In θ solvents[30] $[\eta] = 8.05 \times 10^{-4} M^{0.5}$.

in previous works[9,10] if the molecular weight distributions of the samples are narrow. The transition from the Rouse region to the network region was found to be discontinuous.

If there exists a semidilute region between the two regions and J_e may be scaled in terms of the degree of coil overlapping C/C^* as π and $\eta_R°$, we have

$$J_{eR} \propto (C/C^*)^{1/(1-3\nu)} \propto (C^{1-3\nu}M)^{-1} \quad (6)$$

in semidilute solutions. In good solvents, in which $\nu \simeq 0.6$, eq 6 becomes

$$J_{eR} \propto (C/C^*)^{-1.25} \propto (C^{1.25}M)^{-1} \quad (7)$$

In θ solvents, in which $\nu = 0.50$, we have

$$J_{eR} \propto (C/C^*)^{-2} \propto (C^2M)^{-1} \quad (8)$$

if we assume that eq 6 is valid even in J solvents, as in the case of $\eta°$.[1] Therefore, the concentration dependence of J_e in the semidilute region is expected to be

$$J_e \propto C^{3\nu/(1-3\nu)} \quad (9)$$

and

$$J_e \propto C^{-2.25} \quad \text{in good solvents} \quad (10)$$

$$J_e \propto C^{-3} \quad \text{in θ solvents} \quad (11)$$

The proportionality constants in these relationships are independent of molecular weight.

Since the differences between eq 5 and 7 and between eq 4 and 10 are so slight, very careful experiments covering a wide range of polymer concentration may be required to distinguish between the semidilute and concentrated (network) solutions in good solvents. The boundary between the semidilute and concentrated regions was found at ca. 0.2 g/mL in the case of Π[7] and $\eta°$.[1] The difference between the semidilute and concentrated regions may be more clearly found in θ solvents since the exponent changes from −3 to −2 according to eq 11 and 4.

Applicability of the scaling theory to the elastic properties of polymer solutions was discussed by various authors.[11-14] A number of experimental studies were published on the polymer concentration dependence of J_e. They showed that the polymer concentration dependence of J_e is in the range $J_e \propto C^{-2}$ to $J_e \propto C^{-2.3}$ in the entangled region.[2,3,9-11,14-18] However, most data were obtained at concentrations too high to be used to distinguish the semidilute and network regions. The experiments should be carried out at sufficiently low concentrations of segment by using samples with high molecular weights.

Experimental Section

Linear polystyrenes (PS) having narrow molecular weight distributions obtained from Toyo Soda Manufacturing Co., Ltd., were used in this work. Molecular characteristics of the samples are listed in Table I. It should be noted that the molecular weight distributions of the high molecular weight samples are not as narrow as those of PαMS used in previous works.[1,9,10]

α-Chloronaphthalene (α-CN) and dioctyl phthalate (DOP) were used as good and θ solvents ($T_\theta \simeq 22$ °C), respectively, and were purified by the same method as in previous works.[9,18] Physical properties of these solvents were also previously reported.[9,18]

The original solutions were prepared by mixing weighted amounts of sample and solvent at 50 °C. Methylene chloride (for α-CN mixtures) and cyclohexane (for DOP mixtures) were added to the mixtures to accelerate the dissolution. The solutions were gently stirred a few times per day for about 3 weeks to 2 months until the solutions became uniform. Then methylene chloride and cyclohexane were removed by evaporation in vacuo at 50 °C. Solutions with lower concentrations were prepared by diluting the original solutions by weight. Polymer concentrations were converted to g/mL by assuming the additivity of specific volumes of polymer and solvent.

The measurements were carried out with a Weissenberg rheogoniometer Type R-17 of Sangamo Controls Ltd., equipped with a gap-servo system. A cone-and-plate geometry with a 5-cm diameter and a 4° angle was used. The details and reliability of the measurements with the Weissenberg rheogoniometer Type R-17 were already reported.[19,20] Measurements were carried out at 50 and 20 °C in α-CN and at 30 °C in DOP within an accuracy of ±0.1 °C. A slightly higher temperature than θ (22 °C) was chosen for experimental convenience in DOP. In the measurements with DOP solutions, both the solution and the cone–plate were held at a temperature about 5–10 °C higher than the experimental temperature and then lowered to the experimental temperature.

The zero-shear viscosity $\eta°$ of dilute solutions in toluene at 30 °C was determined by a Maron–Krieger–Sisko type capillary viscometer in the same way as previously.[1]

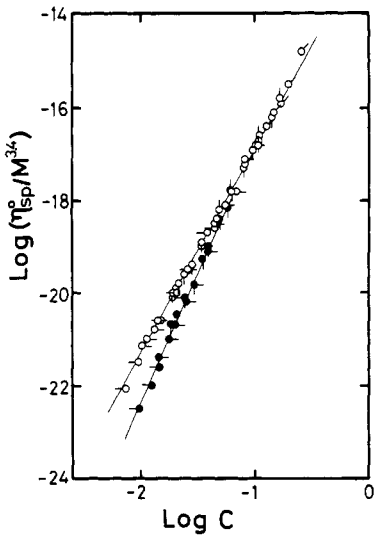

Figure 1. Double-logarithmic plots of $\eta_{sp}°/M^{3.4}$ vs. C in α-CN and DOP. Symbols (○), (○), (○), (○), and (○) and the corresponding filled circles denote the data for samples F-2000, F-850, F-450, F-128, and F-80 in α-CN and DOP, respectively. The solid lines denote the slopes calculated from eq 2 with $\nu = 0.59_5$ for α-CN) and $\nu = 0.53$ (for DOP).

Results

Steady-shear viscosity and compliance were calculated from shear stress and primary normal stress difference observed and extrapolated to the zero-shear rate to obtain the zero-shear viscosity $\eta°$ and the steady-state compliance J_e as described previously.[10] The values of $\eta°$ and J_e thus obtained are listed in Table II.

Figure 1 shows double-logarithmic plots of $\eta_{sp}°/M^{3.4}$ vs. C in α-CN and DOP. In both solvents, $\eta_{sp}°/M^{3.4}$ can be expressed by a universal function of C, as expected from eq 2. The slope of the straight line for α-CN solutions agrees with the value calculated from eq 2, assuming $\nu = 0.59_5$. This value for ν is an average of the values reported

Table II
Steady-Flow Viscosity and Compliance at Zero-Shear Rate

sample code	solvent	T, °C	$C \times 10^2$, g/mL	$\eta°$, P	J_e, cm^2/dyn
F-2000	α-CN	50.0	4.43	3.22×10^4	8.92×10^{-4}
		50.0	3.82	2.25×10^4	1.09×10^{-3}
		50.0	2.69	3.50×10^3	3.24×10^{-3}
		50.0	2.11	1.23×10^3	5.56×10^{-3}
		50.0	1.50	3.15×10^2	1.59×10^{-2}
		50.0	0.96	3.74×10	2.58×10^{-2}
		20.0	0.71	1.83×10	4.77×10^{-2}
F-850	α-CN	50.0	10.12	9.52×10^4	1.16×10^{-4}
		50.0	8.21	4.52×10^4	1.93×10^{-4}
		50.0	6.93	9.35×10^3	3.79×10^{-4}
		50.0	5.52	4.25×10^3	6.80×10^{-4}
		50.0	4.43	1.93×10^3	1.03×10^{-3}
		50.0	3.38	5.94×10^2	1.82×10^{-3}
		50.0	2.60	1.85×10^2	2.76×10^{-3}
		20.0	1.90	8.71×10	5.20×10^{-3}
		20.0	1.43	2.54×10	7.79×10^{-3}
		20.0	1.31	1.77×10	8.60×10^{-3}
		20.0	1.13	9.81×10^0	1.16×10^{-2}
		20.0	1.02	7.18×10^0	1.09×10^{-2}
F-450	α-CN	50.0	14.1	3.99×10^4	1.04×10^{-4}
		50.0	10.6	1.50×10^4	1.45×10^{-4}
		50.0	9.51	8.63×10^3	2.17×10^{-4}
		50.0	7.87	3.60×10^3	2.84×10^{-4}
		50.0	6.35	1.08×10^3	6.15×10^{-4}
		50.0	4.67	2.87×10^2	8.91×10^{-4}
		50.0	3.48	7.80×10	1.41×10^{-3}
		20.0	2.80	4.96×10	2.56×10^{-3}
		20.0	2.39	2.90×10	2.83×10^{-3}
		20.0	2.15	1.91×10	3.10×10^{-3}
		20.0	2.03	1.39×10	3.58×10^{-3}
		20.0	1.91	1.21×10	3.50×10^{-3}
F-128	α-CN	50.0	16.5	1.34×10^3	5.22×10^{-5}
		50.0	11.1	1.81×10^2	1.10×10^{-4}
		50.0	10.6	1.57×10^2	1.46×10^{-4}
		50.0	8.08	4.25×10	1.72×10^{-4}
		50.0	6.15	1.42×10	2.32×10^{-4}
		50.0	4.93	6.39×10^0	2.65×10^{-4}
F-80	α-CN	50.0	25.9	3.05×10^3	2.23×10^{-5}
		50.0	19.4	5.71×10^2	3.05×10^{-5}
		50.0	16.9	2.33×10^2	4.11×10^{-5}
		50.0	14.8	1.29×10^2	4.50×10^{-5}
		50.0	12.6	6.22×10	6.16×10^{-5}
		50.0	10.4	2.88×10	7.45×10^{-5}
		50.0	8.11	1.03×10	8.07×10^{-5}
F-2000	DOP	30.0	1.48	8.04×10^2	2.65×10^{-2}
		30.0	1.27	3.28×10^2	3.22×10^{-2}
		30.0	0.98	9.65×10	5.62×10^{-2}
F-850	DOP	30.0	3.94	1.11×10^4	2.03×10^{-3}
		30.0	2.96	2.13×10^3	4.27×10^{-3}
		30.0	2.54	9.92×10^2	5.98×10^{-3}
		30.0	2.02	2.73×10^2	9.55×10^{-3}
		30.0	1.76	1.46×10^2	1.18×10^{-2}
		30.0	1.46	5.62×10	1.46×10^{-2}
F-450	DOP	30.0	5.80	1.17×10^4	9.23×10^{-4}
		30.0	4.89	6.34×10^3	1.28×10^{-3}
		30.0	3.92	1.62×10^3	2.27×10^{-3}
		30.0	3.45	9.19×10^2	2.49×10^{-3}
		30.0	2.94	2.76×10^2	3.90×10^{-3}
		30.0	2.46	1.31×10^2	5.66×10^{-3}
		30.0	2.06	5.82×10	6.29×10^{-3}
		30.0	1.86	3.63×10	7.19×10^{-3}

for PS solutions in good solvents.[7] In DOP, the slope is a little smaller than the value calculated from eq 2, assuming $\nu = 0.50$, since the experimental temperature was a little higher than the Θ temperature. If we assume $\nu \simeq 0.53$, eq 2 well agrees with the experimental data.

Figure 2 shows double-logarithmic plots of $\eta_R°$ vs. C/C^* in α-CN and DOP. Data in toluene (good solvent) obtained at relatively low concentrations are also added. The experimental points in α-CN and DOP fall on straight lines over wide ranges of C/C^* irrespective of molecular weight. The slopes agree with the values calculated from eq 1, assuming $\nu = 0.59_5$ and 0.53, respectively. The broken line in Figure 2 shows the calculated values of eq 3, assuming $k' = 0.35$. The boundary between the dilute and semidilute regions is in the vicinity of log $(C/C^*) \simeq 0.9$. The good agreement between the experimental and calculated data in α-CN confirms our previous conclusion[1] that the scaling method is useful for predicting the polymer concentration dependence of $\eta°$ in the semidilute region if the molecular weight of the polymers is sufficiently high. The assumption that the concentration dependence of the local frictional coefficient is negligible in the semidilute region appears to be valid. That is, it is certain that all α-CN and DOP solutions employed in this work are in the semidilute region with respect to the behavior of $\eta°$. Here, it should be noted that $\langle S^2 \rangle$ and $[\eta]$ in DOP were calculated from the equations in the footnotes of Table I, that is, from the equations in Θ solvents. Strictly speaking, the equations should be slightly modified, taking into account that ν is not exactly 0.50 but 0.53. The modification may cause a parallel shift of the experimental points for DOP in Figure 2 but no change is required in the above conclusion.

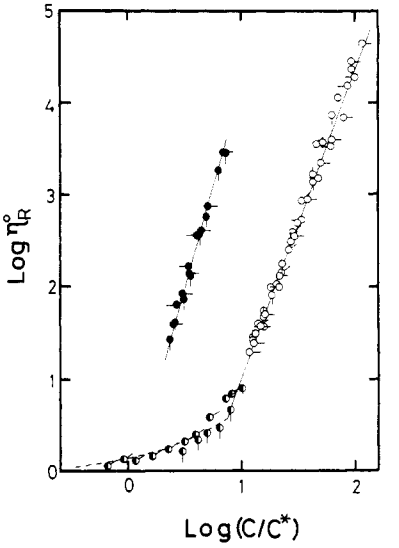

Figure 2. Double-logarithmic plots of viscosity parameter $\eta_R°$ vs. degree of coil overlapping (C/C^*) in α-CN and DOP. The half-filled circles denote the data for dilute solutions in toluene (good solvent) at 30 °C. The other symbols are the same as in Figure 1. The solid lines denote the slopes calculated from eq 1 for α-CN and DOP solutions. The dotted line denotes the calculated values of eq 3 in good solvents, assuming $K' = 0.35$.

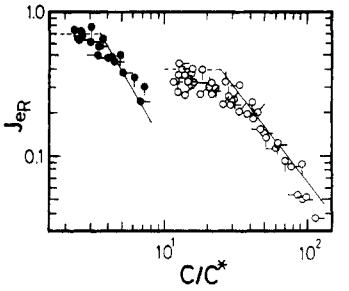

Figure 3. Double-logarithmic plots of the reduced compliance J_{eR} vs. degree of coil overlapping (C/C^*) in α-CN and DOP. Symbols are the same as in Figure 1. The solid lines denote the slope calculated from eq 6 for α-CN and DOP.

In Figure 3, the experimental values of J_e in both α-CN and DOP in Table II are plotted in the form of log J_{eR} vs

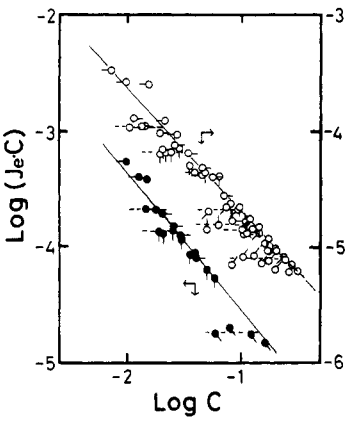

Figure 4. Plots of log ($J_e C$) vs. log C in α-CN and DOP. Symbols (○), (●), and the corresponding filled circles denote the data in α-CN and DOP as reported by Isono et al.[18] The other symbols are the same as in Figure 1.

Table III
Critical Concentration for Network Formation C_2^J

sample code	$M_w \times 10^{-6}$	$C_c^J \times 10^2$, g/mL in α-CN	$C_c^J \times 10^2$, g/mL in DOP
F-850	8.42	2.0_0	1.9_5
F-450	4.48	3.1_6	2.6_3
L-201[a]	1.40	9.1_2	
F-128	1.26	12.0_9	
L-80[a]	0.82_2	13.0_8	13.0_7
F-80	0.77_5	22.0_9	

[a] Original data were reported in ref 18.

log (C/C^*) as predicted from eq 6. The data for α-CN and DOP may be composed of two straight lines; one is a straight horizontal line and the other is a straight line with a slope as predicted from eq 6 ($\nu = 0.59_5$ and 0.53). However, the data are so scattered that the applicability of eq 6 cannot be discussed from this kind of plot. The situation is the same even if we plot the present data in the form of eq 5, that is, of log J_{eR} vs. log (CM). If we compare the present data with the data obtained for PαMS, which have much narrower molecular weight distributions than the present samples, we can point out that this scattering of data is caused by the polydispersities of the present samples.[2,3,21,22]

If we limit our discussion to the polymer concentration dependence of J_e in the semidilute and network regions, the discussion may become free from the effect of molecular weight distribution. The values of J_e in α-CN and DOP, including the data of Isono et al.,[18] are plotted in the form of log ($J_e C$) vs. log C in Figure 4. To compare the data in α-CN with those in DOP, we converted all data in α-CN to the values at 30 °C by multiplying $T\rho/(273 + 30)\rho_0$, where ρ and ρ_0 are the densities of solutions at T and 30 °C, respectively. However, the changes in J_e caused by the conversion are so small that they cannot be observed on the graph. Figure 4 shows that the values of $J_e C$ for all samples at concentrations lower than critical values (C_c^J) appear to be independent of C, whereas the values of $J_e C$ at concentrations higher than C_c^J fit a straight line with a slope of −1.0 to −1.3.

The critical concentration C_c^J evaluated in Figure 4 is listed in Table III and plotted against log M in Figure 5. The slope of this plot is found to be 1.02 ± 0.09 in α-CN. Only three data were obtained in DOP, but there appears to be little difference between the data in α-CN and those in DOP. The solid line in Figure 5 may also be read as the M_c^J–C relationship, in which M_c^J is the corresponding critical molecular weight observed if the molecular weight

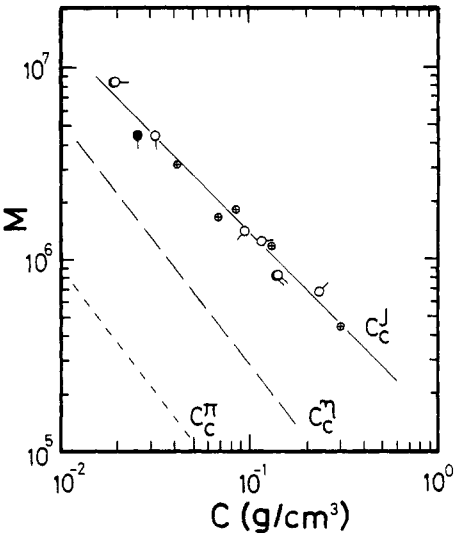

Figure 5. Molecular weight dependence of the critical concentration C_c^J for effective entanglement formation in steady-state compliance J_e. Broken and dotted lines denote the corresponding data in zero-shear viscosity $\eta°$ and osmotic pressure Π in good solvents. Open and filled circles are the same as in Figure 4. Symbol (⊕) denotes the data of C_c^J for PαMS.

is varied, keeping the polymer concentration constant. The region below the line in Figure 5 is the so-called Rouse region, and the region above the line may be the entangled region. The entangled region may be either the network or the semidilute solution. If the entangled region is the "network" solution, we should have

$$C_c^J M = C M_c^J = \text{constant}$$

whereas if the entangled region is the semidilute solution, we would have

$$(C_c^J)^{1.25} M = C^{1.25} M_c^J = \text{constant} \quad \text{(in good solvents)}$$

Sakai et al.[9] reported for PαMS in good solvents that

$$C_c^J M = C M_c^J \simeq 1.35 \times 10^5$$

The present data in Figure 5 show that

$$(C_c^J)^{1.02\pm0.09} M = C^{1.02\pm0.09} M_c^J \simeq 1.4 \times 10^5 \quad (12)$$

in good and Θ solvents. This value is in good agreement with a literature value of M_c^J for the undiluted state (1.3×10^5).[2,3] The data for PαMS by Sakai et al. are also plotted in Figure 5 for comparison.

All data of J_e in the entangled region are double-logarithmically plotted against C in Figure 6. In this figure, all experimental data in good and Θ solvents fit a straight line, respectively. The slope determined by the least-squares method is −2.11 ± 0.01 in α-CN and −2.32 ± 0.03 in DOP. These values may be considerably different from the values predicted from eq 9, i.e., −2.27 ($\nu = 0.59_5$) in α-CN and −2.69 ($\nu = 0.53$) in DOP at 30 °C. Those experimental values appear to be closer to the value (−2.0) predicted from the uniform network model.

Also shown in Figure 6 the values of J_e for the undiluted state and the data reported for highly concentrated solutions of PS. The value for the undiluted state is a simple average of the values in the literature.[17,23,24] Some data in highly concentrated solutions were obtained by Plazek et al.[17] using a creep method, and the other data were estimated from the values of the plateau modulus reported by Isono et al.[25] All the data for high concentrations and melts can be found to exist on the line extrapolated from the present experimental data in both good and Θ solvents. The fact that J_e for the undiluted state is on the line

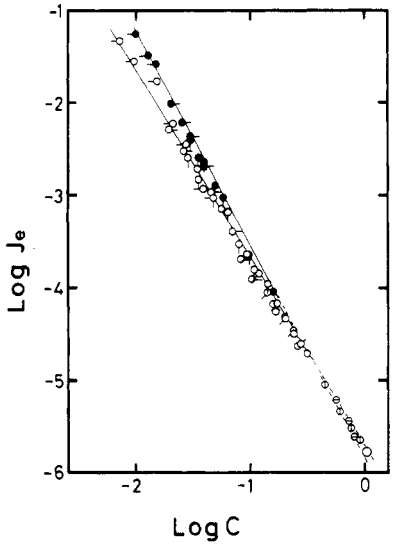

Figure 6. Polymer concentration dependence of J_e in the entangled region. Symbols are the same as in Figure 4. Solid lines were calculated from the present experimental data in α-CN and DOP, using the least-squares method. Symbol (○) denotes the value in undiluted state, while (⊖) and (⊖) denote the data of Plazek et al.[17] and Isono et al.[25] at high concentrations, respectively.

extrapolated from the data in solutions was already reported for various polymers.[9,14,15,17]

If the polymer concentrations are higher than ca. 0.2 g/mL, the solutions are believed to be beyond the semidilute region in viscosity[1] and osmotic pressure.[7] If the semidilute region for J_e exists below 0.2 g/mL, as in the case of $\eta°$ and Π, we should find a crossover point in the vicinity of 0.2 g/mL in α-CN. Although it is not easy to find the crossover point since the change in slope is only −2.27 to −2.0 in α-CN, careful inspection of the data in Figure 6 shows little possibility for the existence of such a crossover point not only in the vicinity of 0.2 g/mL but also in the whole experimental range of the log J_e vs. log C plot in α-CN. If there exists a semidilute region in DOP, the crossover point should be more clearly observed, since the change in the slope is fairly large (from −2.69 to −2.0). In Figure 6, however, no such crossover point can be found in DOP.

Discussion

The present data in good solvent show that there is a great difference between the segment interactions in $\eta°$ and J_e. M_c^J in Figure 5 is generally called the molecular weight between two adjacent entanglement points effective for J_e at a polymer concentration. The corresponding values in viscosity and in osmotic pressure, M_c^η and M_c^Π, in good solvents are also shown for comparison in Figure 5. Here, the M_c^η–C relationship was determined from the data in Figure 2 as

$$M_c^\eta C^{1.27} \simeq 1.5_5 \times 10^4$$

and the M_c^Π–C relationship was estimated from the data in Figure 9 of ref 7 as

$$M_c^\Pi C^{1.27} \simeq 2.4_8 \times 10^3$$

If the critical molecular weights are compared at the same polymer concentration, M_c^J is much larger than M_c^η (and also than M_c^Π), as was previously pointed out.[9] Since the polymer concentration dependence of M_c^J is somewhat different from those of M_c^η and M_c^Π, the ratios M_c^η/M_c^Π and M_c^J/M_c^Π are slightly different at different polymer concentrations. The approximate values of those ratios may be estimated as $M_c^\eta/M_c^\Pi \simeq 6$ and $M_c^J/M_c^\Pi \simeq 25$ in the present experimental range. That is, we have about six thermodynamic blobs between entanglements effective for $\eta°$ and about 25 for J_e. Thus the probability of entanglement formation effective for J_e is much less than that for $\eta°$ for Π. It is understandable that the scaling in terms of a thermodynamic correlation length (eq 6) is not as effective in understading J_e of polymer solutions as in understanding Π and $\eta°$. Although the idea of a semidilute region is surely useful for understanding the polymer concentration and molecular weight dependences of thermodynamic properties (Π) and zero-shear viscosity ($\eta°$) over the entire range of polymer concentration, it is not always useful for all physical properties of polymer solutions.

Thus, it may be concluded that J_e of polymer solutions transfers from the behavior of the Rouse type to that of the network type at a critical polymer concentration as the polymer concentration is increased. To understand the concentration dependence of J_e, the idea of a semidilute region need not be brought in. The uniform network model may be enough for understanding J_e in the entangled region, since the polymer chain between entanglement points is much larger than the thermodynamic correlation length so that the conformation of the chain may be approximated as a Gaussian chain, as pointed out by de Gennes et al.[5,8] The experimental values of the exponent in $J_e \propto C^{-2.11}$ in α-CN and $J_e \propto C^{-2.3}$ in DOP are slightly different from the theoretical value for the uniform network (−2.0). However, such small deviations in exponent may be easily caused by, for example, molecular weight distributions of samples. The theoretical value also may contain some uncertainties for various reasons.

There are some arguments on the application of the scaling method to dynamic behavior of polymer solutions in Θ solvents,[26-28] but in this paper we cannot enter into the problem.

Registry No. Polystyrene (homopolymer), 9003-53-6.

References and Notes

(1) Takahaski, Y.; Isono, Y.; Noda, I.; Nagasawa, M. *Macromolecules* **1985**, *18*, 1002.
(2) Graessley, W. W. *Adv. Polym. Sci.* **1974**, 16.
(3) Ferry, J. D. "Viscoelastic Properties of Polymers"; 3rd ed.; Wiley: New York, 1980.
(4) Flory, P. J. "Principles of Polymer Chemistry" Cornell University Press: Ithaca, NY, 1953.
(5) Daoud, M.; Cotton, J. P.; Farnoux, B.; Jannink, G.; Sarma, G.; Benoit, H.; Duplessix, R.; Picot, C.; de Gennes, P.-G. *Macromolecules* **1975**, *8*, 804.
(6) Noda, I.; Kato, N.; Kitano, T.; Nagasawa, M. *Macromolecules* **1981**, *14*, 668.
(7) Noda, I.; Higo, Y.; Ueno, T.; Fujimoto, T. *Macromolecules* **1984**, *17*, 1055.
(8) de Gennes, P.-G. "Scaling Concepts in Polymer Physics"; Cornell University Press: Ithaca, NY, 1979.
(9) Sakai, M.; Fujimoto, T.; Nagasawa, M. *Macromolecules* **1972**, *5*, 786.
(10) Isono, Y.; Nagasawa, M. *Macromolecules* **1980**, *13*, 862.
(11) Marin, G.; Menezes, E.; Raju, V. R.; Graessley, W. W. *Rheol. Acta* **1980**, *19*, 462.
(12) Adam, M.; Delsanti, M. *J. Phys. (Les Ulis, Fr.)* **1983**, *44*, 1185; **1984**, *45*, 1513.
(13) Osaki, K.; Nishizawa, K.; Kurata, M. *Macromolecules* **1982**, *15*, 1068.
(14) Raju, V. R.; Menezes, E. V.; Marin, G.; Graessley, W. W.; Fetters, L. T. *Macromolecules* **1981**, *14*, 1668.
(15) Nemoto, N.; Odani, H.; Kurata, M. *Macromolecules* **1971**, *4*, 458.
(16) Graessley, W. W.; Masuda, T.; Roovers, J. E. L.; Hadjichristidis, N. *Macromolecules* **1976**, *9*, 127.
(17) Plazek, D. J.; Riande, E.; Markovitz, H.; Raghupathi, N. *J. Polym. Sci., Polym. Phys. Ed.* **1979**, *17*, 2189.
(18) Isono, Y.; Fujimoto, T.; Kajiura, H.; Nagasawa, M. *Polym. J. (Tokyo)* **1980**, *12*, 363.

(19) Endo, H.; Nagasawa, M. *J. Polym. Sci., Part A-2* **1970**, *8*, 371.
(20) Kajiura, H.; Endo, H.; Nagasawa, M. *J. Polym. Sci., Polym. Phys. Ed.* **1973**, *11*, 2371.
(21) Endo, H.; Fujimoto, T.; Nagasawa, M. *J. Polym. Sci., Part A-2* **1971**, *9*, 375.
(22) Kurata, M. *Macromolecules* **1984**, *17*, 895.
(23) Fujimoto, T.; Kajiura, H.; Hirose, M.; Nagasawa, M. *Polym. J. (Tokyo)* **1972**, *3*, 181.
(24) Graessley, W. W.; Roovers, J. E. L. *Macromolecules* **1979**, *12*, 959.
(25) Isono, Y.; Fujimoto, T.; Takeno, N.; Kajiura, H.; Nagasawa, M. *Macromolecules* **1978**, *11*, 888.
(26) Brochard, F.; de Gennes, P.-G. *Macromolecules* **1977**, *10*, 1158.
(27) Brochard, F. *J. Phys. (Les Ulis, Fr.)* **1983**, *44*, 39.
(28) Hecht, A.-M.; Bohidar, H. B.; Geissler, E. *J. Phys., Lett.* **1984**, *45*, 121.
(29) Matsushita, Y.; Noda, I.; Nagasawa, M.; Lodge, T. P.; Amis, E. J.; Han, C. C. *Macromolecules* **1984**, *17*, 1785.
(30) Fukuda, M.; Fukutomi, M.; Kato, Y.; Hashimoto, T. *J. Polym. Sci., Polym. Phys. Ed.* **1974**, *12*, 871.

Calculation of the End-to-End Vector Distribution Function for Short Poly(dimethylsiloxane), Poly(oxyethylene), and Poly(methylphenylsiloxane) Chains

A. M. Rubio

Departamento de Quimica General y Macromoléculas, Facultad de Ciencias, Universidad Nacional de Educación a Distancia, 28040 Madrid, Spain

J. J. Freire*

Departamento de Quimica Fisica, Facultad de Ciencias Quimicas, Universidad Complutense, 28040 Madrid, Spain. *Received January 8, 1985*

ABSTRACT: The end-to-end vector distribution function of short poly(dimethylsiloxane), poly(oxyethylene), and poly(methylphenylsiloxane) chains has been calculated through inference from generalized moments obtained by means of certain iterative equations previously derived. The numerical results obtained this way are tested with Monte Carlo values. A fair agreement is reached in most cases. For the PDMS chain the results are also compared with those calculated with the Hermite series procedure, whose performance is considerably poorer. The main features of the distribution function are analyzed for the different chains. Also, Monte Carlo results showing orientational preferences in the region of small end-to-end distances are reported and discussed.

Introduction

An incisive description of the spatial distribution of a flexible polymer with a finite number of bonds, N, can be accomplished in terms of the end-to-end vector, $\mathbf{R}$, and its density distribution function, $F(\mathbf{R})$, where $\mathbf{R}$ is expressed in a reference frame embedded in the first bonds in the chain.[1] Of course, a high number of bonds provides a Gaussian distribution with spherical symmetry. However, $F(\mathbf{R})$ does not have these properties for short chains, which require detailed numerical calculations based on realistic polymer models. Notwithstanding, the calculations are not routine due to their computational difficulty.

In recent years, the realistic rotational isomeric state model has been adopted to obtain $F(\mathbf{R})$ for a few types of short chains. Thus, results for poly(methylene)[2] (PM), poly(dimethylsiloxane)[3] (PDMS) and polypeptides[4] have been obtained by Flory et al. by means of the Hermite series expansion procedure developed by Flory and Yoon.[1] Nevertheless, these results do not agree in general with those generated by Monte Carlo calculations for the shortest chains, due to the poor convergence of the Hermite series and limitations caused by the lack of efficiency in the evaluation of moments by the usual transfer matrix algorithm. Fixman et al.[5-7] have developed a more powerful method, based on the use of a spherical harmonic representation of rotational operators, to evaluate high moments of $\mathbf{R}$, from which the distribution is inferred through a least-squares algorithm. This method was originally[5,6] aimed at the inference of the end-to-end distance density distribution function $F(\mathbf{R})$, i.e., the radial-dependent part of $F(\mathbf{R})$, and was applicable only to simple "homogeneous" chains such as PM chains. It was subsequently generalized to the calculation of $F(\mathbf{R})$[7,8] by expansion in a spherical harmonic series of the angular coordinates of $\mathbf{R}$. The results obtained this way for PM chains have been satisfactorily compared with values calculated by simulation methods,[7,9] being in good agreement with those values. Moreover, we have performed calculations of moments and radial distribution functions for "heterogeneous" chains, i.e., chains with several different bond lengths, bond angles, or sets of statistical weights for isomers, such as PDMS and poly(oxyethylene) (POE),[10] and also for chains with asymmetric sets of isomers,[11] such as poly(methylphenylsiloxane) (PMPS). These calculations used conveniently modified versions of the original procedure. The results obtained for all these chains are also in good agreement with Monte Carlo values.[10,11]

In this work, we complete the numerical investigation of the generalized inference method by obtaining $F(\mathbf{R})$ for PDMS, POE, and PMPS chains. This study allows us to verify the numerical validity of our quasi-analytical (i.e., nonsimulation) procedure for significantly different types of chain molecules. Moreover, we analyze the variations in symmetry and other properties of these functions for each type of chain. The PDMS results are compared with the values previously obtained by Flory and Chang[3] using the Hermite expansion (we do not know of previously reported attempts to calculate $F(\mathbf{R})$ for the other chains studied here). Numerical values of the components of the persistence vector $\langle \mathbf{R} \rangle$ and the second-moment tensor $\langle \mathbf{R}\mathbf{R}^T \rangle$ are also calculated and analyzed (they are directly related to the "generalized" higher moments needed to infer $F(\mathbf{R})$ as it will be explicitly described in the next

0024-9297/85/2218-2225$01.50/0